YALE JOURNAL OF BIOLOGY AND MEDICINE 98 (2025), pp.21-32. doi: 10.59249/XCAB1680

ORIGINAL CONTRIBUTION

YALE JOURNAL OF BIOLOGY AND MEDICINE
YJBM

Inhibition of p16 and NF-κB Oncogenic Activity in Human Papillomavirus-Infected Cervical Cancer Cells: A New Role for Activating Transcription Factor-3

Zahra Bagheri[a], Haniyeh Abuei[a], Alireza Jaafari[b], Shayan Taki[b], Amirhossein Akbarpour Arsanjani[a], and Ali Farhadi[a,c,*]

[a]Division of Medical Biotechnology, Department of Medical Laboratory Sciences, School of Paramedical Sciences, Shiraz University of Medical Sciences, Shiraz, Iran; [b]School of Medicine, Shiraz University of Medical Sciences, Shiraz, Iran; [c]Diagnostic Laboratory Sciences and Technology Research Center, School of Paramedical Sciences, Shiraz University of Medical Sciences, Shiraz, Iran

Objective: Activating transcription factor 3 (ATF3) has attracted recent scientific attention as a novel mediator of tumor suppression, particularly within the context of cervical cancer (CC). Our prior research demonstrated that ATF3 overexpression induces cell cycle arrest and apoptosis in human papillomavirus (HPV)16- and HPV18-positive CC cells. The present study aims to examine the impact of ATF3 overexpression on the expression levels of p16 and NF-κB, two proteins with pro-tumorigenic roles in HPV-induced CC. **Methods**: Ca Ski and HeLa cells underwent transfection with pCMV6-AC-IRES-GFP plasmids containing the *ATF3* gene. To establish the optimal plasmid DNA quantities for transfection, MTT assay was conducted. Furthermore, fluorescence microscopy and flow cytometric analysis were employed to assess the efficiency of transfection. The expression levels of p16 and NF-κB were evaluated by RT-qPCR and western blotting prior and subsequent to ATF3 overexpression. **Results**: The overexpression of ATF3 induced a decrease in *p16* mRNA levels in both Ca Ski and HeLa cells ($p<0.04$), along with the concomitant reduction of p16 protein expression within both cellular populations ($p<0.005$). Additionally, it led to a reduction in NF-κB p65 protein levels in both cell lines ($p<0.005$), with no discernible impact on its mRNA expression. **Conclusion**: Given ATF3's demonstrated capability to downregulate p16 and NF-κB, both of which play important pro-tumorigenic roles in HPV-related CC, ATF3 emerges as a promising therapeutic candidate with the potential for application in the treatment of CC.

*To whom all correspondence should be addressed: A. Farhadi, PhD, Email: Farhadi_a@sums.ac.ir; ORCID: https://orcid.org/0000-0002-2271-670X.

Abbreviations: ATF3, Activating transcription factor 3; CC, Cervical cancer; HPV, Human papillomavirus; CDK4/6, Cyclin dependent kinase 4 and 6; pRb, Retinoblastoma; IL1A, Interleukin-1A; NF-κB, Nuclear factor kappa B; AP1, Activator protein 1.

Keywords: ATF3, p16, NF-κB, HPV, cervical cancer

Author Contributions: ZB: experimentation and data analysis. HA: methodology, data validation, and original draft preparation. AJ: statistical analysis, data interpretation, and review. ST and AAA: methodology. AF: conceptualization, supervision, review, and editing. All authors reviewed the manuscript and approved the submission of the article.

INTRODUCTION

The cyclin-dependent kinase inhibitor p16 (p16) is a well-studied tumor suppressor that exerts its function through the inhibition of cyclin dependent kinase 4 and 6 (CDK4/6) [1]. CDK4/6 are responsible for the inactivation of the retinoblastoma tumor suppressor protein (pRb) by its phosphorylation [2]. As a result, the phosphorylated pRb can no longer perform its function of blocking G1/S transition. p16 transcription is usually repressed by epigenetic means in normal cells [3]; however, it can be induced by several oncogenes as a cell defense mechanism [4,5]. Despite the tumor suppressor role of p16 in most cellular contexts, it appears that high expression of p16 induced by human papillomavirus (HPV) 16 E7 oncoprotein exhibits an oncogenic role and is required for the survival of HPV-infected cells [6]. This is probably due to the ability of HPV16 E7 oncoprotein to target pRb for proteasomal degradation [7]. In the absence of pRb, a substrate of CDK4/6, cell tolerance for the activity of CDK4/6 is compromised since there are other CDK4/CDK6 substrates that should stay in an unphosphorylated state when pRb is inactivated in order for the cell to survive [8-10]. Accordingly, the continued expression of p16 induced by HPV16 E7 oncoprotein is essential to inactivate the CDK4/6 to prevent the phosphorylation of such CDK4/6 substrates in HPV E7-expressing cells [6]. In greater detail, in HPV-infected cervical cancer (CC) cells with inactivated pRb, CDK6 can potentially phosphorylate and inactivate HuR, a pivotal factor that functions to stabilize interleukin-1A (*IL1A*) mRNA and prolong its half-life and, as a result, promote the proliferation of CC cells. Elevated p16 levels in these cells serve to inactivate CDK6, thereby impeding the inactivation of HuR and promoting IL1A stabilization, ultimately favoring proliferation in CC cells [11].

Nuclear factor kappa B (NF-κB) is a transcription factor that plays a crucial role in regulating the expression of numerous genes involved in cell survival, cell proliferation, immune response, and inflammation [12]. There are five members of the NF-κB protein family in mammals: p65 (RelA), RelB, c-Rel, p50 (NF-κB1), and p52 (NF-κB2) [13]. All of these members have to form homo- or heterodimers in order to become activated and translocated to the cell nucleus [14]. The most common form of activated NF-κB is the p50/p65 heterodimer [15]. The constitutive activation of NF-κB has been observed in several human malignancies including CC, resulting in increased cell survival and resistance to apoptosis which can contribute to tumor growth, progression, and resistance to treatment [16-19]. Accordingly, inhibition of NF-κB could be a promising focus for cancer treatment.

Activating transcription factor 3 (ATF3) belongs to the larger family of ATF/cAMP response element-binding (CREB) transcription factors and participates in various cellular and physiological processes including cell differentiation, apoptosis, stress responses, and the regulation of inflammatory responses [20]. The dual role of ATF3 in tumor suppression and cancer progression is complex and context-dependent, varying across different cancer types. In some cases, ATF3 functions as a tumor suppressor by inhibiting metastasis and regulating critical signaling pathways, while in other contexts, it can promote cancer progression, particularly through its involvement in stress responses [21]. For instance, ATF3 has been shown to suppress bladder cancer cell migration by upregulating gelsolin, which remodels the actin cytoskeleton and reduces metastatic potential [22]. In clear cell renal cell carcinoma (ccRCC), ATF3 inhibits tumor growth by deactivating the EGFR/AKT/GSK3β/β-catenin signaling pathway, which is crucial for cell proliferation and invasion [23]. Conversely, in colorectal cancer, ATF3 promotes resistance to ferroptosis by regulating cystathionine β-synthase (CBS) during cystine deprivation, thereby facilitating cancer cell survival and progression [24]. Additionally, ATF3 plays a role in inflammatory responses and oxidative stress, both of which can contribute to tumorigenesis when dysregulated [25]. While ATF3 exhibits tumor-suppressive properties, its ability to promote cancer progression underscores the complexity of its functions, suggesting that its effects are highly dependent on the specific tumor microenvironment and cellular context.

Our previous studies indicated that the overexpression of ATF3 in Ca Ski and HeLa CC cells resulted in cell cycle arrest and apoptosis [26,27]. Furthermore, we formerly demonstrated that ATF3 overexpression led to a significant reduction of NF-κB protein level in Ca Ski cells. Herein, we aim to examine whether the ectopic overexpression ATF3 can reduce the expression of p16 and NF-κB mRNA and protein in HPV16/18-infected CC cells.

METHODS

Cell Culture and Transfection

HeLa and Ca Ski cells were purchased from the national cell bank of Iran (NCBI Code: C115, Pasteur Institute, Tehran, Iran) and the American Type Culture Collection (ATCC; Manassas, VA, USA), respectively. For culturing the HeLa cells, RPMI-1640 medium, and for the Ca Ski cells, Dulbecco's modified Eagle's medium (DMEM) was used. Both cell lines were cultured in complete growth media with 10% fetal bovine serum (FBS), and 1% penicillin-streptomycin (all Sigma-Aldrich; USA) and incubated in 37°C with 5% CO2. Following 24 h of growth, HeLa and Ca Ski cells were

transfected with pCMV6-AC-IRES-GFP recombinant plasmids containing the *ATF3* gene (pCMV6-ATF3) and pCMV6-AC-IRES-GFP without the *ATF3* gene (mock), which were available from a previous study [28]. For this purpose, both cell lines were seeded in 6-well cell culture plates with the concentration of 8×10^5 cells per well. Once the cells had reached the density of 60-70%, they were transfected with pCMV6-ATF3 plasmids using lipofectamine 3000 (Thermo Fisher Scientific, Waltham, MA, USA) according to the manufacturer's protocol. The cells were washed with PBS and cultured in fresh media 4-6 h after transfection. Additionally, the untreated cell groups were maintained under the same conditions as the experimental groups but were not subjected to any specific treatment.

Fluorescence Microscopy and Flow Cytometry Analysis

Transfection efficiency was assessed using fluorescence microscopy and transmission light microscopy (Olympus, Japan). Transfected cells were directly observed using an Olympus microscope with a 20-fold objective lens at 24, 48, and 72 h post-transfection. Fluorescent images were captured using the GFP filter cube. To measure the efficiency of transfection, the number of total cells and the cells expressing GFP was counted. At each time point, five images were captured and assessed individually. Flow cytometric analysis was conducted 24, 48, and 72 h post-transfection. Briefly, the cells were washed with PBS and subsequently detached from the cell culture plate by trypsin-EDTA solution. Afterwards, the cells were centrifuged at 350 g for 5 min and resuspended in PBS for fluorescent intensity evaluation using a FACS-Calibur flow cytometry instrument (BD Biosciences; San Jose, California, USA). A total of 10 000 cells underwent analysis in each experiment. The data were analyzed using FlowJo software version 10.0 (FlowJo LLC; USA).

Cytotoxicity Assay

MTT assay was employed to assess the cytotoxicity of ATF3. In brief, HeLa and Ca Ski cells were seeded into 96-well culture plates at the density of 8000 cells per well in 200 µL of their corresponding media and incubated at 37°C and 5% CO2. Once the cells had reached the confluence of 70%, they underwent transfection with different amounts of pCMV6-ATF3 and mock plasmid ranging from 0.1 to 1 µg according to the previously mentioned transfection protocol. Cell viability was examined 24, 48, and 72 h post-transfection by adding fresh medium supplemented with 20 µL of MTT solution (5 mg/mL) (Sigma-Aldrich; USA), followed by a 4-hour incubation for crystal formation. Subsequently, 150 µL of DMSO (Sigma-Aldrich; USA) was introduced into each well and the absorbance was determined at the wavelength of 570 nm using Sat Fax 2100 microplate reader (Stat Fax; USA). The MTT assay was conducted in triplicate.

Cell Lysis and Protein Assay

HeLa and Ca Ski cells were seeded into 6-well culture plates and incubated at 37°C and 5% CO2 overnight. Afterwards, the cells were transfected as described previously. After 72 h, the cells were harvested, washed with cold PBS, and sonicated (Amplitude: 80–100, 2 × 30 s, with 30-s cooling intervals) in RIPA buffer (1% Triton X100, 0.1% SDS, 150 mM NaCl, 50 Mm Tris-HCl, pH 8.0) containing 25 µL of protease inhibitor cocktail (Sigma-Aldrich; USA). Then, the samples were centrifuged at 15 000 g and 4°C for 20 min and the supernatants were collected. Finally, Bradford protein assay (Bio-Rad Bradford protein assay) was employed to determine the protein concentration of test and control cells by generating an absorbance standard curve.

ATF3, p16, and NF-kB Western Blotting Analysis

The cell lysate obtained from the previous step was mixed with a 5× sample buffer containing 0.25 M Tris-HCl pH 6.8, 50% glycerol, 10% SDS, 0.1% bromophenol blue, and 5% β-mercaptoethanol, and subsequently boiled at 95°C for 10 min. Afterwards, equal amounts of protein from each sample were subjected to electrophoresis in a 12% SDS-polyacrylamide gel and transferred onto polyvinylidene fluoride (PVDF) membranes (Millipore, Feltham, UK) using Bio-Rad Mini Trans-Blot® electrophoretic transfer cell at 300 mA for 3 h. The membranes were incubated in a blocking solution containing 5% skim milk and 0.05% Tween 20 for 16 h and then washed for 15 min with TBST buffer (150 mMNaCl, 50 mM Tris-base, and 0.05% Tween 20). The quantities of ATF3, p16, and NF-κB protein were measured using monoclonal anti-ATF3, anti-p16, and anti-NF-κB (p65) antibodies (1:500, Santa Cruz Biotechnologies, Santa Cruz, CA, USA). β-actin (1:5000, Santa Cruz Biotechnologies, Santa Cruz, CA, USA) served as an internal control. After three rounds of washing with TBST, the membranes were incubated with a horseradish peroxidase-conjugated secondary antibody (1:10000, Sigma-Aldrich; USA) at room temperature for 2 h. Subsequently, they were washed with TBS buffer (50 mM Tris-base and 150 mM NaCl) twice. Then, 10 mL 3,3′-Diaminobenzidine (DAB) substrate (Sigma-Aldrich; USA) (5 mg of DAB in 10 mL DDW) supplemented with 5 µl H2O2 was added to the PVDF surface. Finally, the reaction was stopped using DDW.

Table 1. Oligonucleotide Primer Sequences Used for Reverse-Transcription Real-Time PCR Assay

Gene	Sequence (5' to 3')	PCR product size (bp)	Annealing temperature (°C)
p16-Forward	ACCAGAGGCAGTAACCATG	128	58.5
p16-Reverse	CCTGTAGGACCTTCGGTGAC		
NF-κB-Forward	TAGGAAAGGACTGCCGGGA	100	59
NF-κB-Reverse	CCGCTTCTTCACACACTGGA		
ATF3-Forward	GAGTGCCTGCAGAAAGAGT	117	58
ATF3-Reverse	CCGATGAAGGTTGAGCATG		

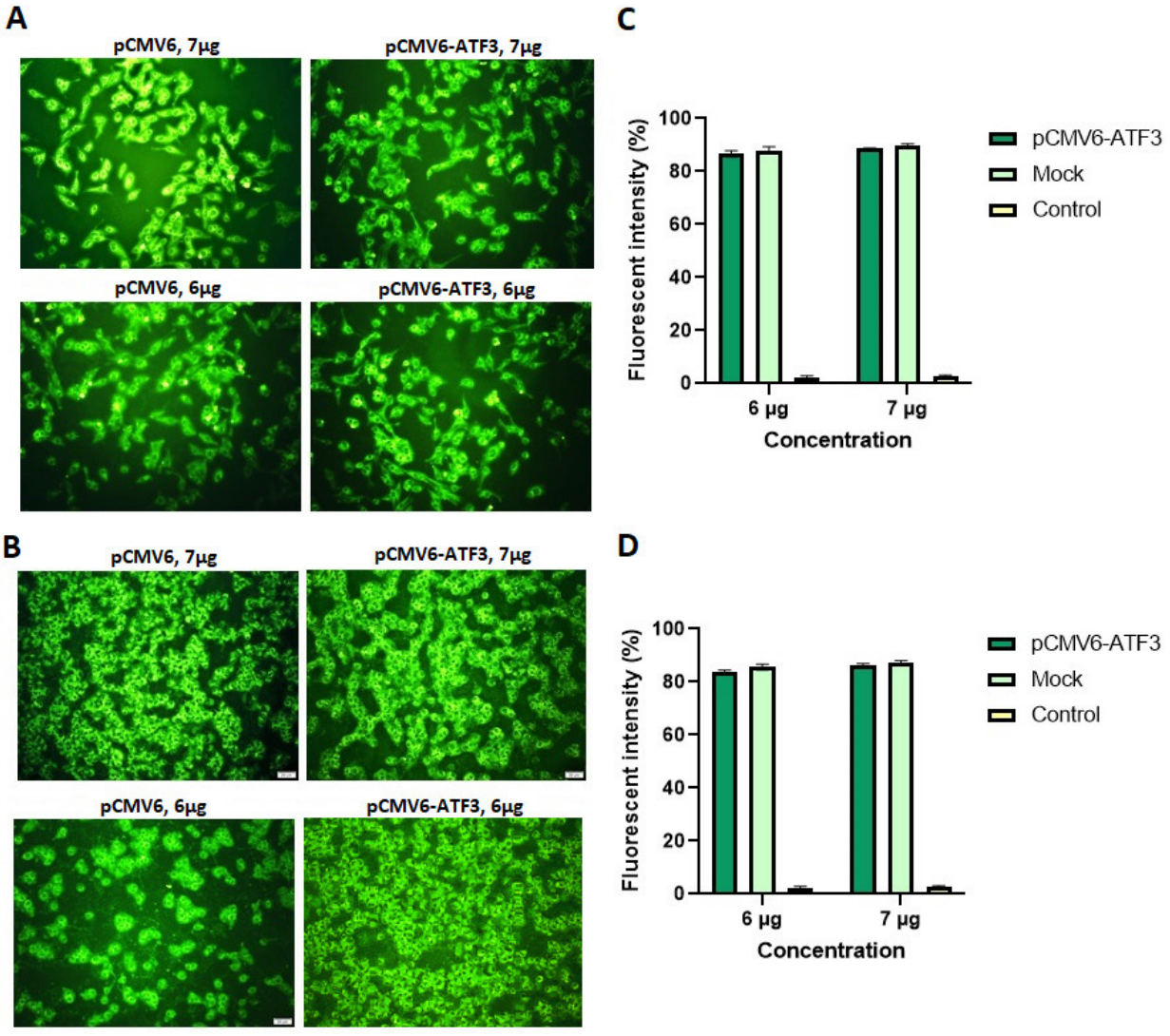

Figure 1. **Fluorescent intensity of pCMV6-ATF3-transfected, mock-transfected, and control groups using fluorescence microscopy and flow cytometry**. The fluorescence microscope results showed that the percentage of transfected cells with pCMV6-ATF3 and pCMV6 was more than 85% for both HeLa (**A**) and Ca Ski (**B**) cells at 72 h post-transfection. (Zoom in: 20 µm). The flow cytometry analysis showed that the average transfection efficiency using 7 µg pCMV6-ATF3 after 72 h was 87.83% for HeLa (**C**) and 85.12% for Ca Ski (**D**) cells. Mock: cells transfected with pCMV6 without ATF3; control: untransfected cells.

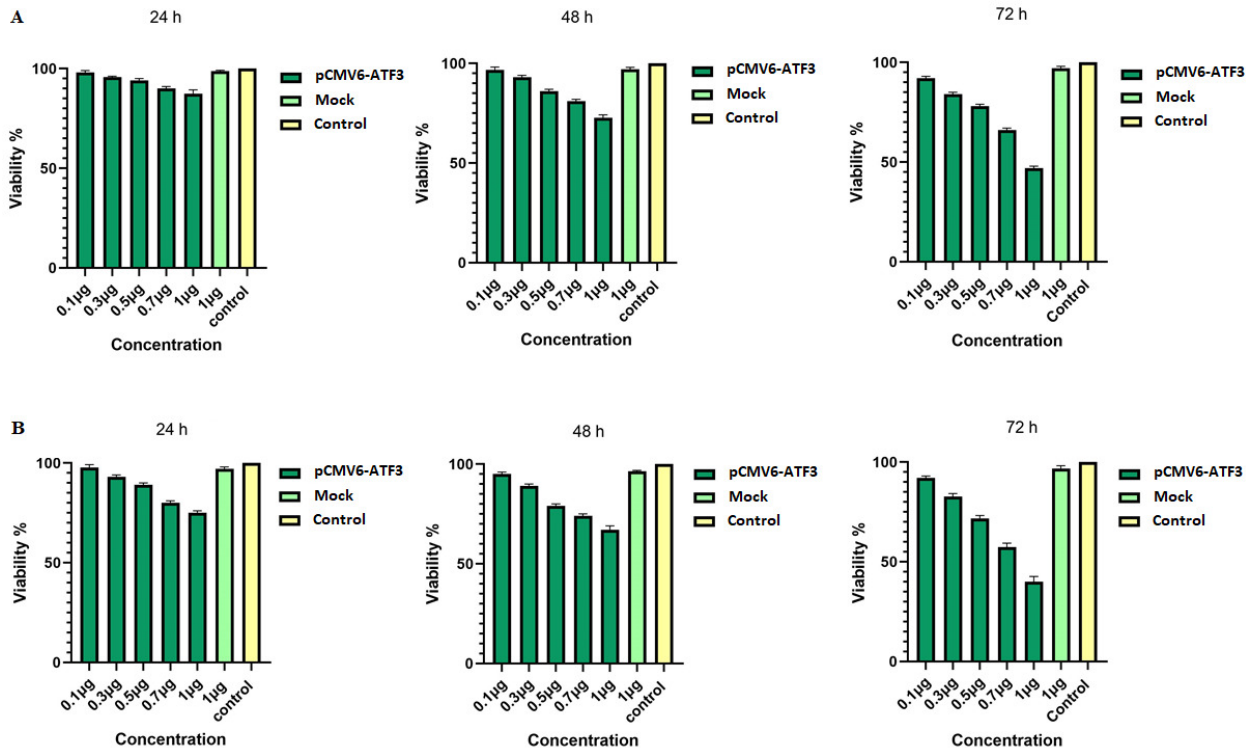

Figure 2. **Viability assay of HeLa (A) and Ca Ski cells (B) transfected with pCMV6-ATF3 plasmids**. In comparison with the untreated group, a statistically significant reduction in the viability of HeLa and Ca Ski cells was observed 24 h post-transfection when the concentrations of 1 µg and 0.7 µg of pCMV6-ATF3 plasmid had been used, respectively ($p<0.01$). The initial concentrations of pCMV6-ATF3 plasmids eliciting significant reductions in the cell viability of both cell lines at 48 and 72 h post-transfection were 0.5 and 0.3 µg, respectively ($p<0.01$). No significant reduction in the viability of mock-transfected cells was observed ($p>0.05$).

Reverse Transcription Quantitative PCR (RT-qPCR)

The primer sequences employed in RT-qPCR were designed using Gene Runner 3.0 software (accessible at http://www.generunner.net/) and are listed in Table 1. Total RNA extraction from the cultured cells was conducted using RiboEx TM kit (GeneAll, Korea), followed by cDNA synthesis at 37°C for 15 min using the PrimeScript RT reagent kit (TaKaRa, Japan). RT-qPCR was carried out using the ABI Prism 7000 Sequence Detection System (Applied Biosystems, Foster City, CA, USA) and the RealQ Plus 2x Master Mix Green (Ampliqon, Denmark). To assess primer efficiency, standard curves were established for each primer set. The relative fold changes of the target genes were calculated by following the Pfaffl method [29], with *GAPDH* serving as the housekeeping gene (Forward: GGCCTCCAAGGAGTAAGACC, Reverse: AGGGGTCTACATGGCAACTG) [30]. The thermocycling protocol consisted of an initial denaturation at 95°C for 15 min, followed by 40 cycles of 95°C for 15 sec, annealing temperature (58.5°C and 59°C for p16 and NF-κB, respectively) for 30 sec, and 72°C for 20 sec.

Statistical Analysis

Statistical analysis was conducted using Statistical Package for the Social Sciences (SPSS) software version 22 (IBM Corp. Released 2013. IBM SPSS Statistics for Windows, Version 22.0. Armonk, NY: IBM Corp.). The results were presented as mean ± SD. Given the non-normal distribution of the data, the Kruskal-Wallis test, a non-parametric method suitable for comparing multiple independent groups with non-normal data, was employed to assess the significance of mean differences between the groups. A p-value of less than 0.05 was considered statistically significant.

RESULTS

Transfection of Recombinant Vectors into HeLa and Ca Ski Cells

Increasing the quantity of DNA for transfection resulted in an elevation in the fluorescent intensity of the cells, reaching a plateau when 7 µg DNA was employed for the transfection of HeLa and Ca Ski cells. Beyond this point, there was no further alteration in the propor-

tion of transfected cells. Cellular analysis was conducted 24, 48, and 72 h post-transfection. Thereafter, fluorescent microscope images of the transfected cells were acquired and used to manually calculate the efficiency of transfection by counting both transfected and total cells, with the efficiency being determined as the ratio of the former to the latter. The percentage of cells successfully transfected with pCMV6-ATF3 exceeded 85% for both HeLa and Ca Ski cells at 72 h post-transfection. Additionally, mock-transfected HeLa and Ca Ski cells exhibited transfection efficiencies exceeding 88%. Employing flow cytometry analysis, the mean transfection efficiency was determined to be 87.83% for HeLa and 85.12% for Ca Ski cells at 72 h post-transfection (Figure 1).

MTT Assay

The viability of HeLa and Ca Ski cells following transfection with pCMV6-ATF3 was assessed using MTT assay. Cells were treated with pCMV6-ATF3 at varying DNA concentrations ranging from 0.1 to 1 μg, and the mock plasmid at a 1 μg concentration for 24, 48, and 72 h. The MTT assay demonstrated that the overexpression of ATF3 at the concentration of 1 μg led to the maximum inhibition of cell growth in both HeLa and Ca Ski cells (56% and 63%, respectively at 72 h) with significant differences compared to untreated and mock-transfected counterparts ($p<0.0005$) (Figure 2).

Western Blotting

The overexpression of ATF3 in transfected HeLa and Ca Ski cells was verified through western blot analysis. The analysis demonstrated a significant increase in the expression of ATF3 protein in pCMV6-ATF3-transfected cells compared to untreated and mock-transfected counterparts ($p<0.001$). Furthermore, the levels of ATF3, p16, NF-κB, and β-actin proteins were assessed in untreated, mock-transfected, and pCMV6-ATF3-transfected groups. As depicted in Figure 3, the results of western blot analysis also revealed a significant reduction in the levels of p16 and NF-κB proteins in HeLa and Ca Ski cells when compared to the control cell groups ($p<0.005$).

RT-qPCR

At the mRNA level, RT-qPCR analysis conducted 72 h post-transfection demonstrated that elevated *ATF3* gene expression in transfected HeLa and Ca Ski cells resulted in a significant reduction in *p16* gene expression ($p<0.04$). However, the overexpression of ATF3 had no significant effect on NF-κB mRNA expression ($p>0.05$) in HeLa and Ca Ski cells when compared to the control and mock-transfected groups. The summarized results detailing gene expression alterations in pCMV6-ATF3-transfected, mock-transfected, and control cells are presented in Figure 4.

DISCUSSION

Despite the tumor suppressor role of p16 in most cells, it is well-established that p16 exhibits oncogenic activity in HPV-transformed CC cells, in which HPV oncoprotein E7 mediates the degradation of pRb protein [6,11]. This oncogenic activity of p16 depends on its ability to inhibit CDK4/CDK6 since in the absence of pRb, active CDK4/CDK6 can phosphorylate other substrates that should stay in an unphosphorylated state in order for the cell to survive [6]. High-level p16 expression has been suggested not only as a valuable biomarker and prognostic factor in HPV-transformed cervical cells, but a promising target for cancer therapy since high p16 expression is exclusively essential for the survival of CC cells, but not normal cells, making these cells favorably vulnerable to targeting treatments [11]. Downregulation of p16 in CC cells has been shown to induce cell cycle arrest in the G1 phase and inhibit cell proliferation [31]. Additionally, p16 silencing resulted in the upregulation of p53, pRb, and p21 in CC cells and a significantly higher rate of apoptosis when the cells were exposed to DNA damage stress, including cisplatin treatment and UV irradiation [32].

Previous investigations, including our own, have demonstrated that ectopic overexpression of ATF3, a versatile transcription factor commonly exhibiting downregulation in CC, induces G1 cell cycle arrest and apoptosis in CC cell lines, Ca Ski, and HeLa [26,27,33]. It has been proposed that ATF3 might inhibit p53 ubiquitination mediated by the HPV-16 E6 oncoprotein, thereby preventing its subsequent proteasomal degradation. This potential inhibitory effect could result from ATF3 competing with E6-associated protein for binding to HPV-16 E6 [34]. Moreover, ATF3 has exhibited a direct interaction with p53, contributing to the stabilization of p53 and the prevention of its ubiquitination [35]. However, a previous study of ours indicated that the tumor suppressor activity of ATF3 in HPV-18-infected CC cells was p53-independent [26]. Herein, we investigated the impact of ATF3 overexpression on the expression of p16 in Ca Ski and Hela cells. Our results demonstrated that the ectopic overexpression of ATF3 in HPV16- and HPV18-positive CC cells led to a significant decrease in both mRNA and protein expression of p16.

ATF3 binds to DNA in the form of either a homodimer or a heterodimer in conjunction with members of the Jun family of proteins, such as C-Jun and Jun-B [36]. These dimeric complexes, collectively recognized as the transcription factor activator protein 1 (AP1), can bind to AP1-binding DNA sequences [37]. Within the p16 promoter, there exist three AP1-binding sites through which

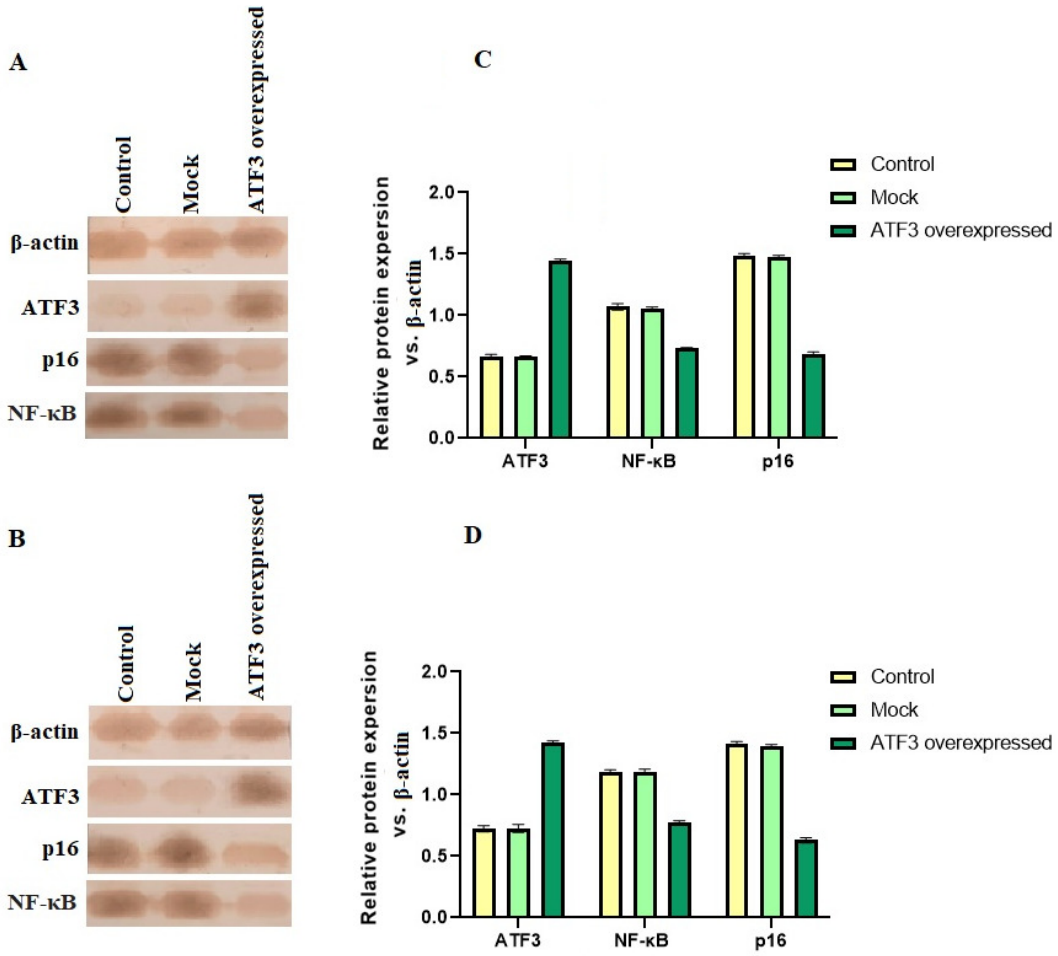

Figure 3. **ATF3, p16, and NF-κB protein levels in HeLa (A) and Ca Ski cells (B)**. Densitometry analysis of the relative levels of protein expression after 72 h in pCMV6-ATF3-transfected HeLa (**C**) and Ca Ski (**D**) cells exhibited higher expression of ATF3 compared to the untreated and mock-transfected groups ($p<0.001$). The results of western blotting also demonstrated that the overexpression of ATF3 had a significant effect on p16 and NF-κB protein levels in HeLa and Ca Ski cells when compared to the untreated and mock-transfected cells ($p<0.005$). The uncropped images are provided in Appendix A: Supplemental Figure 1.

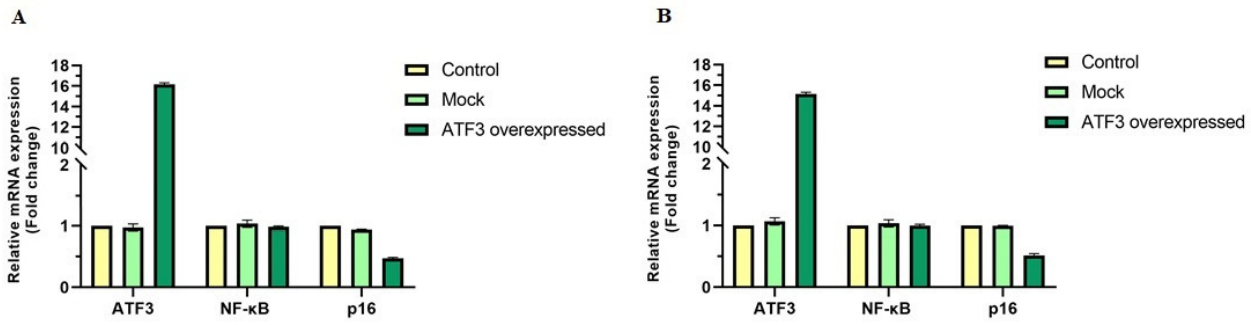

Figure 4. **The relative expression of *ATF3*, *p16*, and *NF-κB* mRNA in HeLa (A) and Ca Ski (B) cells by RT-qPCR**. ATF3 overexpression decreased *p16* mRNA expression ($p<0.04$) but had no significant effect on NF-κB mRNA expression ($p>0.05$) in comparison with the mock-transfected and control groups.

these dimers exert direct regulatory control over p16 expression [38]. A previous study has documented that a specific AP1 dimer consisting of C-Jun and Jun-B elicited a downregulation of both promoter activity and p16 expression in nasopharyngeal carcinoma cells [39]. In accordance with the observed data, it is plausible that ATF3 could regulate *p16* gene expression through its binding to the AP1-binding sites positioned within the gene's promoter. Furthermore, the downregulation of p16 expression by ATF3 may contribute to the apoptotic and G1 arrest effects observed in HPV-positive CC cells overexpressing ATF3. Additional investigation including electrophoretic mobility shift assay (EMSA) and Super-EMSA is recommended to confirm the binding of ATF3 to AP1-binding sites within the p16 promoter.

NF-κB is known as a transcription factor with a bilateral role within the context of cancer. On the one hand, the activation of NF-κB induces an inflammatory response intended to eliminate the cancerous cells [40]. On the other hand, the constitutive activation of NF-κB in various types of cancer generates a spectrum of pro-tumorigenic functionalities [41]. Upon infection, HPV induces the downregulation of NF-κB, consequently dampening the immune response and facilitating the progression of HPV infection into a persistent phase [42]. However, NF-κB undergoes constitutive activation throughout the progression of CC [19], enabling it to induce the transcription of the genes involved in cell proliferation and those implicated in metastasis, angiogenesis, and cell immortality [42]. Consequently, the inhibition of NF-κB may offer a therapeutic approach for the treatment of CC.

In our previous investigation, we demonstrated that the overexpression of ATF3 resulted in the downregulation of NF-κB p65 protein in HPV16-positive CC cells [27]. Herein, we conducted RT-qPCR in order to elucidate whether ATF3's influence on NF-κB *p65* downregulation occurs via a reduction in its gene expression. Our findings revealed no evidence of ATF3 impacting on the expression levels of NF-κB *p65* mRNA in either of the cell lines. However, when ATF3 was overexpressed in HeLa cells, a consistent outcome was observed, marked by the downregulation of NF-κB p65 protein. Previous investigations have shown that ATF3 is capable of direct interaction with the p65 subunit of NF-κB, resulting in its negative regulation [43]. Furthermore, HPV oncoproteins E6 and E7 have been shown to upregulate p65 protein levels, and knocking down these viral oncogenes is associated with the downregulation of p65 expression solely at the protein level, without altering mRNA levels [44]. Similarly, in our study, the overexpression of ATF3 resulted in a reduction in p65 protein levels exclusively, while leaving its mRNA expression unaffected. This observation may suggest that ATF3's interaction with the E6 protein could disrupt E6-mediated mechanisms that enhance NF-κB signaling. For example, ATF3 might prevent E6 from promoting the ubiquitination and degradation of negative regulators of the NF-κB pathway, such as cylindromatosis lysine 63 deubiquitinase [45], or from inactivating the X-box binding protein [46]. However, further research is required to confirm the precise mechanism through which ATF3 regulates p65 protein levels.

Targeting ATF3 offers a promising approach to enhancing CC treatment, particularly when combined with existing chemotherapeutic strategies. ATF3 plays a critical role in mediating apoptosis and cellular stress responses, making it a valuable target for improving the effectiveness of current therapies. Research by St Germain et al. demonstrated that ATF3 enhances the cytotoxic effects of cisplatin when used alongside histone deacetylase (HDAC) inhibitors like M344. This combination not only increases ATF3 expression but also correlates with higher rates of tumor cell apoptosis. Interestingly, M344-induced ATF3 expression occurs independently of MAPK pathways, suggesting alternative regulatory mechanisms that could be therapeutically exploited [47]. Additionally, combining ATF3 modulation with agents such as IL6-type cytokines may further sensitize CC cells to chemotherapeutics like etoposide, potentially through the STAT3/IRF1 pathway [48]. ATF3 is also involved in regulating cancer stemness and epithelial-to-mesenchymal transition (EMT), which could help overcome treatment resistance in CC [49]. However, ATF3's dual roles in inflammation and apoptosis introduce complexities that could affect treatment outcomes. Therefore, further preclinical and *in vivo* studies are essential to fully understand ATF3's therapeutic potential and refine its application in CC therapies. Given the significant role of NF-κB in both inflammation and cancer, further exploration of how ATF3 modulates NF-κB could provide valuable insights into whether its effects are driven by oncogenic signaling or immune modulation. To investigate ATF3's interactions with these pathways in greater detail, techniques such as co-immunoprecipitation are needed to provide mechanistic insights into how ATF3 regulates protein stability and degradation. These insights could be crucial for developing therapeutic strategies that exploit the regulatory pathways of ATF3.

The findings of this study related to ATF3, p16, and NF-κB expression in HPV-positive CC cells may have implications for other HPV-associated cancers, such as head and neck squamous cell carcinomas (HNSCCs). For instance, high p16 overexpression strongly correlates with HPV DNA positivity in HPV-driven HNSCCs, particularly in oropharyngeal squamous cell carcinoma (OPSCC) [50]. Additionally, HPV-positive HNSCCs exhibit NF-κB overactivity [51]. Furthermore, Xu et al. reported that ATF3 exerts anti-tumor functions in tongue squamous cell carcinoma (TSCC), likely by negatively

regulating the expression of interferon alpha inducible proteins 6 (IFI6) and 27 (IFI27) [52]. Collectively, these findings suggest that the functions of ATF3, p16, and NF-κB in HPV-positive CC may extend to HPV-associated HNSCCs and potentially other HPV-driven cancers. In contrast, in HPV-negative tumors, the expression of these genes may not confer the same regulatory or protective effects, potentially contributing to the more aggressive behavior observed in HPV-negative HNSCCs. A deeper understanding of ATF3, p16, and NF-κB functions and their downstream signaling pathways could provide novel therapeutic opportunities for HPV-positive tumors.

CONCLUSION

Our current investigation provides evidence for the role of ATF3 in modulating the transcription and protein expression of p16 in HPV-positive CC cells. Additionally, ATF3 appears to influence the reduction of NF-κB p65 protein levels. These findings suggest that ATF3 may play a role in regulating cell proliferation in CC, highlighting its potential as a therapeutic target. However, further investigation is required to fully elucidate its therapeutic potential and mechanism of action.

Acknowledgements: We would like to acknowledge Philip Novy for readability edits.
Funding: This study was supported by a grant from Shiraz University of Medical Sciences, Shiraz, Iran, under the Agreement No. 23560.
Availability of Data and Materials: All data generated during this study are included in this published article.
Ethical Approval: The research project has been approved by the Ethics Committee of Shiraz University of Medical Sciences (Approval ID: IR. SUMS. REC.1400.331).
Competing Interests: The authors declare that they have no competing interests.

REFERENCES

1. Hara E, Smith R, Parry D, Tahara H, Stone S, Peters G. Regulation of p16CDKN2 expression and its implications for cell immortalization and senescence. Mol Cell Biol. 1996 Mar;16(3):859–67.
2. Connell-Crowley L, Harper JW, Goodrich DW. Cyclin D1/Cdk4 regulates retinoblastoma protein-mediated cell cycle arrest by site-specific phosphorylation. Mol Biol Cell. 1997 Feb;8(2):287–301.
3. Popov N, Gil J. Epigenetic regulation of the INK4b-ARF-INK4a locus: in sickness and in health. Epigenetics. 2010;5(8):685–90.
4. Agger K, Cloos PA, Rudkjaer L, Williams K, Andersen G, Christensen J, et al. The H3K27me3 demethylase JMJD3 contributes to the activation of the INK4A-ARF locus in response to oncogene- and stress-induced senescence. Genes Dev. 2009 May;23(10):1171–6.
5. Barradas M, Anderton E, Acosta JC, Li S, Banito A, Rodriguez-Niedenführ M, et al. Histone demethylase JMJD3 contributes to epigenetic control of INK4a/ARF by oncogenic RAS. Genes Dev. 2009 May;23(10):1177–82.
6. McLaughlin-Drubin ME, Park D, Munger K. Tumor suppressor p16INK4A is necessary for survival of cervical carcinoma cell lines. Proc Natl Acad Sci USA. 2013 Oct;110(40):16175–80.
7. Gonzalez SL, Stremlau M, He X, Basile JR, Münger K. Degradation of the retinoblastoma tumor suppressor by the human papillomavirus type 16 E7 oncoprotein is important for functional inactivation and is separable from proteasomal degradation of E7. J Virol. 2001 Aug;75(16):7583–91.
8. Anders L, Ke N, Hydbring P, Choi YJ, Widlund HR, Chick JM, et al. A systematic screen for CDK4/6 substrates links FOXM1 phosphorylation to senescence suppression in cancer cells. Cancer Cell. 2011 Nov;20(5):620–34.
9. Liu F, Matsuura I. Inhibition of Smad antiproliferative function by CDK phosphorylation. Cell Cycle. 2005 Jan;4(1):63–6.
10. Matsuura I, Denissova NG, Wang G, He D, Long J, Liu F. Cyclin-dependent kinases regulate the antiproliferative function of Smads. Nature. 2004 Jul;430(6996):226–31.
11. Li M, Yang J, Liu K, Yang J, Zhan X, Wang L, et al. p16 promotes proliferation in cervical carcinoma cells through CDK6-HuR-IL1A axis. J Cancer. 2020 Jan;11(6):1457–67.
12. Hayden MS, West AP, Ghosh S. NF-kappaB and the immune response. Oncogene. 2006 Oct;25(51):6758–80.
13. Baldwin AS Jr. Series introduction: the transcription factor NF-kappaB and human disease. J Clin Invest. 2001 Jan;107(1):3–6.
14. Wong D, Teixeira A, Oikonomopoulos S, Humburg P, Lone IN, Saliba D, et al. Extensive characterization of NF-κB binding uncovers non-canonical motifs and advances the interpretation of genetic functional traits. Genome Biol. 2011 Jul;12(7):R70.
15. Chen FE, Huang DB, Chen YQ, Ghosh G. Crystal structure of p50/p65 heterodimer of transcription factor NF-kappaB bound to DNA. Nature. 1998 Jan;391(6665):410–3.
16. Karin M. Nuclear factor-kappaB in cancer development and progression. Nature. 2006 May;441(7092):431–6.
17. Li Q, Withoff S, Verma IM. Inflammation-associated cancer: NF-kappaB is the lynchpin. Trends Immunol. 2005 Jun;26(6):318–25.
18. Branca M, Giorgi C, Ciotti M, Santini D, Di Bonito L, Costa S, et al.; HPV-Pthogen ISS Study Group. Upregulation of nuclear factor-kappaB (NF-kappaB) is related to the grade of cervical intraepithelial neoplasia, but is not an independent predictor of high-risk human papillomavirus or disease outcome in cervical cancer. Diagn Cytopathol. 2006 Aug;34(8):555–63.
19. Nair A, Venkatraman M, Maliekal TT, Nair B, Karunagaran D. NF-kappaB is constitutively activated in high-grade squamous intraepithelial lesions and squamous cell carcinomas of the human uterine cervix. Oncogene. 2003 Jan;22(1):50–8.
20. Jadhav K, Zhang Y. Activating transcription factor 3 in immune response and metabolic regulation. Liver Res. 2017 Sep;1(2):96–102.
21. Ku HC, Cheng CF. Master regulator activating transcrip-

tion factor 3 (ATF3) in metabolic homeostasis and cancer. Front Endocrinol (Lausanne). 2020 Aug;11:556.
22. Yuan X, Yu L, Li J, Xie G, Rong T, Zhang L, et al. ATF3 suppresses metastasis of bladder cancer by regulating gelsolin-mediated remodeling of the actin cytoskeleton. Cancer Res. 2013 Jun;73(12):3625–37.
23. Gao S, Gao L, Wang S, Shi X, Yue C, Wei S, et al. ATF3 suppresses growth and metastasis of clear cell renal cell carcinoma by deactivating EGFR/AKT/GSK3β/β-catenin signaling pathway. Front Cell Dev Biol. 2021 Mar;9:618987.
24. Liu J, Lu X, Zeng S, Fu R, Wang X, Luo L, et al. ATF3-CBS signaling axis coordinates ferroptosis and tumorigenesis in colorectal cancer. Redox Biol. 2024 May;71:103118.
25. Liu S, Li Z, Lan S, Hao H, Baz AA, Yan X, et al. The Dual Roles of Activating Transcription Factor 3 (ATF3) in Inflammation, Apoptosis, Ferroptosis, and Pathogen Infection Responses. Int J Mol Sci. 2024 Jan;25(2):824.
26. Kooti A, Abuei H, Farhadi A, Behzad-Behbahani A, Zarrabi M. Activating transcription factor 3 mediates apoptotic functions through a p53-independent pathway in human papillomavirus 18 infected HeLa cells. Virus Genes. 2022 Apr;58(2):88–97.
27. Akbarpour Arsanjani A, Abuei H, Behzad-Behbahani A, Bagheri Z, Arabsolghar R, Farhadi A. Activating transcription factor 3 inhibits NF-κB p65 signaling pathway and mediates apoptosis and cell cycle arrest in cervical cancer cells. Infect Agent Cancer. 2022 Dec;17(1):62.
28. Kooti A, Abuei H, Jaafari A, Taki S, Saberzadeh J, Farhadi A. Activating transcription factor 3 mediates apoptosis and cell cycle arrest in TP53-mutated anaplastic thyroid cancer cells. Thyroid Res. 2024 Aug;17(1):12.
29. Pfaffl MW. A new mathematical model for relative quantification in real-time RT–PCR. Nucleic acids research. 2001;29(9):e45-e. https://doi.org/10.1093/nar/29.9.e45.
30. Guenzle J, Wolf LJ, Garrelfs NW, Goeldner JM, Osterberg N, Schindler CR, et al. ATF3 reduces migration capacity by regulation of matrix metalloproteinases via NFκB and STAT3 inhibition in glioblastoma. Cell Death Discov. 2017 Feb;3(1):17006.
31. Zhang CY, Bao W, Wang LH. Downregulation of p16(ink4a) inhibits cell proliferation and induces G1 cell cycle arrest in cervical cancer cells. Int J Mol Med. 2014 Jun;33(6):1577–85.
32. Lau WM, Ho TH, Hui KM. p16INK4A-silencing augments DNA damage-induced apoptosis in cervical cancer cells. Oncogene. 2007 Sep;26(41):6050–60.
33. Oh YK, Lee HJ, Jeong MH, Rhee M, Mo JW, Song EH, et al. Role of activating transcription factor 3 on TAp73 stability and apoptosis in paclitaxel-treated cervical cancer cells. Mol Cancer Res. 2008 Jul;6(7):1232–49.
34. Wang H, Mo P, Ren S, Yan C. Activating transcription factor 3 activates p53 by preventing E6-associated protein from binding to E6. J Biol Chem. 2010 Apr;285(17):13201–10.
35. Yan C, Lu D, Hai T, Boyd DD. Activating transcription factor 3, a stress sensor, activates p53 by blocking its ubiquitination. EMBO J. 2005 Jul;24(13):2425–35.
36. Hai TW, Liu F, Coukos WJ, Green MR. Transcription factor ATF cDNA clones: an extensive family of leucine zipper proteins able to selectively form DNA-binding heterodimers. Genes Dev. 1989 Dec;3(12B 12b):2083–90.
37. Hai T, Curran T. Cross-family dimerization of transcription factors Fos/Jun and ATF/CREB alters DNA binding specificity. Proc Natl Acad Sci USA. 1991 May;88(9):3720–4.
38. Passegué E, Wagner EF. JunB suppresses cell proliferation by transcriptional activation of p16(INK4a) expression. EMBO J. 2000 Jun;19(12):2969–79.
39. Song X, Ai M, Chen X, Deng X, Tao Y, Gong J, et al. Regulation of c-Jun/JunB heterodimers mediated by Epstein-Barr virus encoded latent membrane protein 1 on p16. Chin Sci Bull. 2004;49(7):676–83.
40. Disis ML. Immune regulation of cancer. J Clin Oncol. 2010 Oct;28(29):4531–8.
41. Smyth MJ, Dunn GP, Schreiber RD. Cancer immunosurveillance and immunoediting: the roles of immunity in suppressing tumor development and shaping tumor immunogenicity. Adv Immunol. 2006;90:1–50.
42. Tilborghs S, Corthouts J, Verhoeven Y, Arias D, Rolfo C, Trinh XB, et al. The role of Nuclear Factor-kappa B signaling in human cervical cancer. Crit Rev Oncol Hematol. 2017 Dec;120:141–50.
43. Kwon JW, Kwon HK, Shin HJ, Choi YM, Anwar MA, Choi S. Activating transcription factor 3 represses inflammatory responses by binding to the p65 subunit of NF-κB. Sci Rep. 2015 Sep;5(1):14470.
44. Gu NJ, Wu MZ, He L, Wang XB, Wang S, Qiu XS, et al. HPV 16 E6/E7 up-regulate the expression of both HIF-1α and GLUT1 by inhibition of RRAD and activation of NF-κB in lung cancer cells. J Cancer. 2019 Nov;10(27):6903–9.
45. An J, Mo D, Liu H, Veena MS, Srivatsan ES, Massoumi R, et al. Inactivation of the CYLD deubiquitinase by HPV E6 mediates hypoxia-induced NF-kappaB activation. Cancer Cell. 2008 Nov;14(5):394–407.
46. Xu M, Katzenellenbogen RA, Grandori C, Galloway DA. NFX1 plays a role in human papillomavirus type 16 E6 activation of NFkappaB activity. J Virol. 2010 Nov;84(21):11461–9.
47. St Germain C, O'Brien A, Dimitroulakos J. Activating Transcription Factor 3 regulates in part the enhanced tumour cell cytotoxicity of the histone deacetylase inhibitor M344 and cisplatin in combination. Cancer Cell Int. 2010 Sep;10(1):32.
48. Walch-Rückheim B, Pahne-Zeppenfeld J, Fischbach J, Wickenhauser C, Horn LC, Tharun L, et al. STAT3/IRF1 pathway activation sensitizes cervical cancer cells to chemotherapeutic drugs. Cancer Res. 2016 Jul;76(13):3872–83.
49. Khan AQ, Hasan A, Mir SS, Rashid K, Uddin S, Stienhoff M, editors. Exploiting Transcription Factors to Target EMT and Cancer Stem Cells for Tumor Modulation and Therapy. Elsevier; 2024. https://doi.org/10.1016/j.semcancer.2024.03.002.
50. Bhardwaj S, Gitman M, Ramirez JD, Paniz-Mondolfi A, Westra WH. Reappraisal of p16 for Determining HPV Status of Head and Neck Carcinomas Arising in HPV Hotspots. Am J Surg Pathol. 2024 May;48(5):581–7.
51. Schrank TP, Prince AC, Sathe T, Wang X, Liu X, Alzhanov

DT, et al. NF-κB over-activation portends improved outcomes in HPV-associated head and neck cancer. Oncotarget. 2022 May;13(1):707–22.
52. Xu L, Zu T, Li T, Li M, Mi J, Bai F, et al. ATF3 downmodulates its new targets IFI6 and IFI27 to suppress the growth and migration of tongue squamous cell carcinoma cells. PLoS Genet. 2021 Feb;17(2):e1009283.

Appendix A

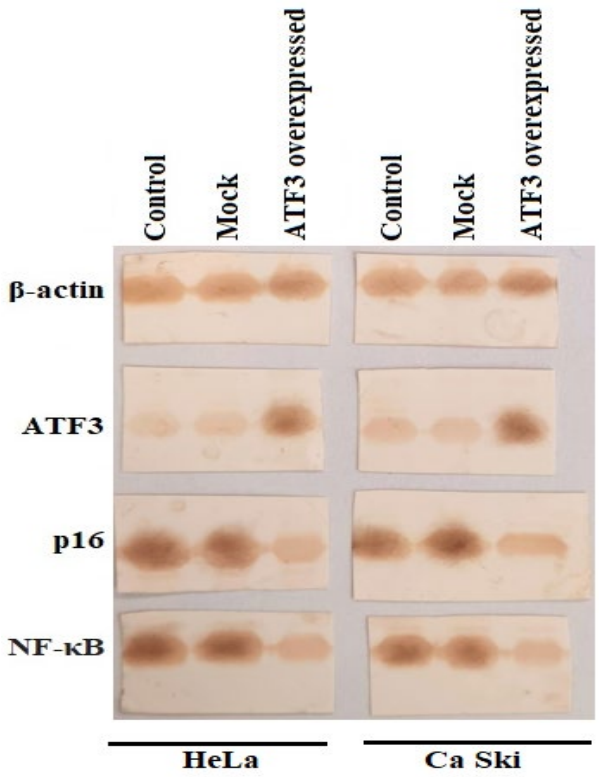

Supplemental Figure 1. HeLa and Ca Ski cells were transfected with pCMV6-ATF3 plasmid. Mock-transfected and untreated cells were employed as controls. After 72 h, ATF3, p16, and NF-κB protein levels were determined in HeLa and Ca Ski cells by western blotting. Whole cell lysates were subjected to western blotting with anti-ATF3, anti-p16, anti-NF-κB, and anti- β-actin antibodies.